MATERIALS SCIENCE

High-speed transport of liquid droplets in magnetic tubular microactuators

Wenwei Lei[1]*, Guanglei Hou[2]*, Mingjie Liu[1,3]*, Qinfeng Rong[1], Yichao Xu[1,3], Ye Tian[2]†, Lei Jiang[1,2,3]

Magnetic field–induced droplet actuation has attracted substantial research interest in recent years. However, current magnetic-controlled liquids depend primarily on magnetic particles added to a droplet, which serves as the actuator on an open surface. These liquids inevitably suffer from droplet splitting with the magnetic particles or disengaging with the magnet, possibly leading to sample contamination, which severely limits their transport speed and practical applications. Here, we report a simple and additive-free method to fabricate magnetic tubular microactuators for manipulating liquid droplets by magnetism-induced asymmetric deformation, which generates an adjustable capillary force to propel liquids. These magnetic tubular microactuators can drive various liquid droplets with controllable velocity and direction. A speed of 10 cm s^{-1} can be achieved, representing the highest speed of liquid motion driven by an external stimulus–induced capillary force in a closed tube found so far.

INTRODUCTION

The controlled manipulation of small amounts of liquid has attracted substantial research interest (*1*–*6*). From the perspectives of scientific research and practical application, the control of fluid stream or droplet is extremely important, especially for the fields of biosensing (*7*), medical diagnostics (*8*), drug delivery (*9*, *10*), and "lab-on-a-chip" DNA purifications (*11*). Thus far, there have been many reports on actuating liquid droplets with external thermal gradients, light, electric fields, and magnetic fields (*12*–*16*). Magnetic actuation is recognized as one promising method for liquid actuation based on its several advantages, including long-range action, large control forces, and weak interaction between the magnetic field and the liquid droplet. However, to the best of our knowledge, almost all previous reports on the magnetic manipulation of droplet used magnetic particles added to the droplet as the actuator on an open surface (*2*, *17*–*19*). These methods inevitably suffer from droplet splitting with the magnetic particles or disengaging with the magnet, possibly leading to sample contamination and substantially limiting their potential use in general applications.

The self-propelled motion of a droplet is generally achieved by droplet asymmetry caused by a chemical reaction, a temperature gradient, or an asymmetric geometry (*20*, *21*). For example, drops in tapered tubes can self-propel toward the narrow region because of the Laplace pressure gradient (*21*, *22*). These self-propelled droplet motions can occur only when the pinning force is negligible compared to the driving force induced by the wettability gradient or the Laplace pressure gradient. Because the pinning force depends on the degree of contact angle hysteresis (CAH), it can be overcome by designing tubular microactuators. Recently, Lv *et al.* (*23*) reported a strategy to manipulate fluid slugs by photoinduced asymmetric deformation of cross-linked liquid crystal polymer tubular microactuators, which induces capillary forces that can be used for liquid propulsion. Although this is a remarkable method for designing tubular microactuators, its relatively low transport speed, requirement for specific materials, and complex preparation process severely restrict its application in real life.

To resolve these limitations, here, we report a simple and reliable method for fast liquid transport by using asymmetric magnetic tubular microactuators (MTMAs). The MTMAs are prepared from a novel designed magnetic polydimethylsiloxane (PDMS) base soft tube, showing asymmetric deformation in a magnetic field (Fig. 1A). The deformation of the upper part of the tube is induced by the magnetic field, which leads to asymmetric deformation with respect to the tube section containing the liquid droplet. As the magnet moves, this asymmetric deformation takes the shape of a dynamic conical tube, producing a Laplace pressure gradient that induces forward liquid transport. The MTMAs move droplets toward the narrower end, overcoming CAH via the asymmetric deformation of the tube induced by the magnetic field. The speed of partially wetting liquids reaches 10 cm s^{-1}, which is the highest speed of liquid motion driven by an external stimulus–induced capillary force in closed tubular microactuators found so far. Because our microactuators do not require the addition of any magnetic-sensitive particles into liquids, various liquid droplets can be successfully manipulated in the MTMA with controllable velocity and direction and can even run uphill. As far as we know, this is the first investigation into the magnetic on-demand actuation of an additive-free liquid in a closed channel.

RESULTS

Fabrication of MTMAs

MTMAs were fabricated from low-cost cross-linked PDMS and magnetic carbonyl iron powder. A simple preparation approach for MTMAs is shown in fig. S1. This approach includes two PDMS curing processes. First, pure PDMS (Sylgard 184, Dow Corning) was thoroughly mixed with the curing reagent at a weight ratio of 10:1. Then, the mixture was coated on steel capillaries with different outer diameters, which were maintained vertically at room temperature for different duration times, followed by thermal curing at 60°C for 20 min. From the above step, we can obtain a uniform PDMS steel capillary. Second, ferromagnetic iron (Fe) particles were doped in PDMS prepolymer with vigorous stirring to form a mixture. Then, the mixture was coated on a clean glass slide using the tape-casting method to form a thickness of approximately 100 μm. The previously obtained PDMS

[1]Key Laboratory of Bio-Inspired Smart Interfacial Science and Technology of Ministry of Education, School of Chemistry, Beihang University, Beijing 100191, P. R. China. [2]Key Laboratory of Bio-Inspired Materials and Interfacial Science, Technical Institute of Physics and Chemistry, Chinese Academy of Sciences, Beijing 100190, P. R. China. [3]Beijing Advanced Innovation Center for Biomedical Engineering, Beihang University, Beijing 100191, P. R. China.
*These authors contributed equally to this work.
†Corresponding author. Email: tianyely@iccas.ac.cn

steel capillary was carefully placed on the magnetic PDMS layer, covering the capillary with a thin layer of magnetic PDMS, and then thermally cured at 80°C for 60 min. A low temperature and a short time for curing were used in the first curing process, allowing the two PDMS layers to combine very well without delamination. Last, the completely cured PDMS steel capillary was swelled in hexane and then quickly demolded. Following the optimization of the combinations of different capillaries and magnetic stripe thicknesses (figs. S2 and S3), the wall thicknesses of the nonmagnetic stripe area and the magnetic strip were chosen at approximately 110 and 70 μm, respectively, for further study. Figure S4 illustrates that the magnetic stripe can be well combined with the PDMS capillary.

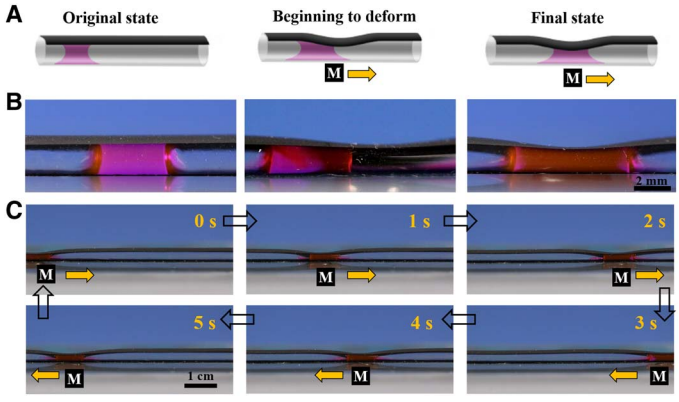

Fig. 1. Design of MTMAs. (**A**) Schematics showing the motion of a liquid droplet of wetting liquid confined in an MTMA driven by a magnetic field. (**B**) Side views of the corresponding instantaneous state of the liquid droplet in the obtained MTMAs. (**C**) Lateral photographs of the magnetic-induced motion of an ethanol droplet in an MTMA fixed on a substrate. The magnet moves from left to right. The ethanol droplet is propelled toward the right; when the direction of the magnet is reversed (bottom row), the direction of movement of the droplet is also reversed (movie S1).

Driving liquid droplets in MTMAs by asymmetric deformation

Asymmetrical deformation is crucial for building tubular microactuators that induce a capillary force for propelling liquids. Side views of the instantaneous states (original state, begin to deform, final state) of a liquid droplet in the obtained MTMAs are shown in Fig. 1B. Because of the wetting property with a CA of 25.8 ± 2.4° on the PDMS surface in the air, a partially wetting liquid (ethanol, dyed by rhodamine B) in the tube can form a very clear concave surface. Under a magnetic field (a cylindrical magnet with a diameter of 4 mm and a surface magnetic field intensity of 0.5 T), the ethanol deformed with the MTMA in an asymmetric manner, and these MTMAs can thus successfully manipulate liquid motion with a magnet (Fig. 1C and movie S1).

The deformation of MTMAs with different diameters under a magnetic field is shown in fig. S5 (B to D). The degree of deformation is potentiated as increasing the diameter. There was little deformation when the diameter was less than 0.8 mm, but noticeable deformation

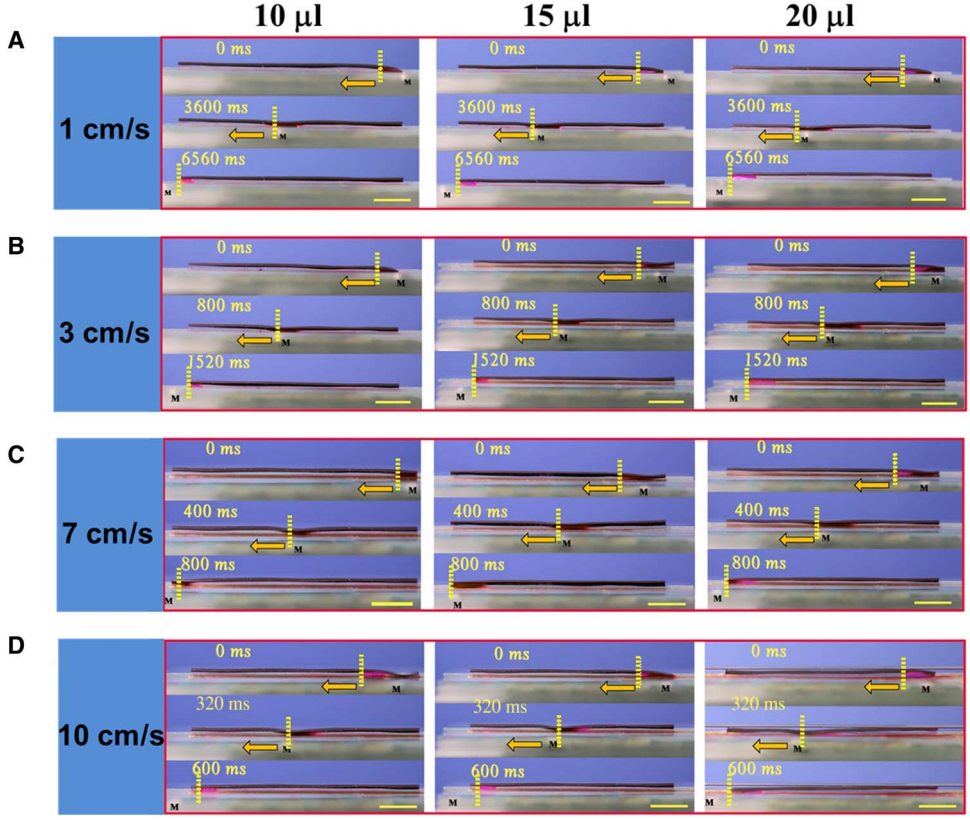

Fig. 2. Optical images showing magnetic-controlled motion of ethanol. Each parallel row shows the results for a different magnet speed, and the yellow arrows denote the magnet movement direction. (**A**) 1 cm s^{-1}. (**B**) 3 cm s^{-1}. (**C**) 7 cm s^{-1}. (**D**) 10 cm s^{-1}. In each column, there is a different liquid volume: 10, 15, and 20 μl. The ethanol droplets can be propelled without disengagement from the magnet. Scale bars, 1 cm (movie S2).

could be observed when the diameter is increased to 2.0 mm. This is consistent with the fact that tubes with smaller diameter are more difficult to deform (*24*, *25*). Unless stated otherwise, the MTMAs used in this work were prepared with a diameter of 2.0 mm. When the droplet deformed with the MTMA due to the magnetic force, the resultant asymmetric deformation constituted a minimum opening angle of approximately 4° (fig. S5F). In the absence of a liquid drop (fig. S5G), the deformation induced by the magnetic force produces a maximum opening angle of approximately 10°. Therefore, with the uniform movement of the magnet, the continuous deformation of the MTMAs forms a dynamic conical capillary, which generates an adjustable capillary force to propel liquids toward the narrower end.

Propelling different volume liquid droplets at different velocities in MTMAs

Recent efforts have been directed toward the use of various external stimuli (such as thermal gradients, light, electric fields, and chemicals) for liquid transport. Although each of these methods has unique advantages, the major obstacle they all encounter is hysteresis forces (*26*). Hysteresis forces often lead to deceleration and stagnation of the droplet. Therefore, for conventional methods, the typical transport speeds of the liquid droplet (ranging from μm s^{-1} to mm s^{-1}) are often too slow for practical applications in real life (*27*). However, our MTMAs can successfully surmount this problem. As shown in Fig. 2, the transport process of a liquid (ethanol, dyed by rhodamine B) with different volumes was recorded using a digital camera. When the magnet underneath the droplet was moved at a speed of 1 cm s^{-1}, the ethanol droplet can be propelled slowly with the continuous deformation of MTMA. When we increased the volume of the ethanol droplet from 10 to 25 μl, the droplet still moved with the magnet (Fig. 2A and movie S2). Furthermore, the speed of the magnet is increased from 4 to 10 cm s^{-1}, and both a small droplet (10 μl) and a large droplet (25 μl) can move at a constant speed with the magnet, rather than disengage from the magnet (Fig. 2, B to D, and movie S2). This behavior indicates that the MTMA can provide a sufficient driving force to overcome the hysteresis forces for liquid droplet movement with high velocity. Upon further increases in the speed of the magnet, the instantaneous magnetic force cannot induce the deformation of the MTMA (*28*–*30*). We also consider other factors that can affect the movement of the droplets, such as the diameter of the tube, the addition of magnetic nanoparticles to the tube, and the strength of the magnet. The effects of these factors on the movement of droplets are shown in fig. S6, which can help us further apply these MTMAs on demand. The movement speed of the ethanol reaches 10 cm s^{-1}, which is the highest speed reported thus far in the literature for a droplet moving in tubular microactuators at room temperature. A detailed comparison is provided in table S1. The present method achieves the highest speed and has several other advantages in preparation materials, energy consumption, and little sample contamination (*15*, *18*, *23*, *31*–*35*).

Various liquid droplets propelled by magnetic forces in MTMAs

Because these MTMAs do not require the addition of any magnetic-sensitive particles in the driven liquids, various liquid droplets could

Table 1. Properties of various probe liquids collected from the literature or through laboratory testing. The light blue area represents the conditions that droplets can be driven in MAMTs by the magnetic force, while the light yellow area represents the conditions that droplets cannot be driven in MAMTs by the magnetic force.

Parameter / Probe liquid	Contact angle θ (°)	Advancing angle θ_A (°)	Receding angle θ_R (°)	Contact angle hysteresis Δθ (°)	Surface tension* (mN/m)	Viscosity* (mPa·s)
1,2-Dichloroethane	33.3 ± 1.5	83.9 ± 1.3	75.9 ± 1.4	8.0 ± 0.1	35.43	0.84
Butyl alcohol	32.4 ± 1.8	82.3 ± 2.1	75.2 ± 1.8	7.1 ± 0.3	24.42	2.94
Isopropanol	19.7 ± 2.0	63.7 ± 1.6	58.2 ± 1.5	5.5 ± 0.1	23.64	2.4
Ethyl acetate	35.6 ± 2.3	76.3 ± 2.1	66.8 ± 1.9	9.5 ± 0.2	27.95	0.426
Hexadecane	16.7 ± 2.0	52.3 ± 1.8	46.1 ± 1.6	6.2 ± 0.2	27.6	3.34
Ethanol	25.8 ± 1.8	67.3 ± 2.2	60.5 ± 1.8	6.8 ± 0.4	23.57	1.07
Ethanol:Water (80)†	41.7 ± 2.5	95.3 ± 1.8	80.2 ± 2.0	15.1 ± 0.2	27.51‡	1.96‡
Ethanol:Water (70)†	52.6 ± 1.3	102.4 ± 1.5	85.1 ± 1.6	17.3 ± 0.1	29.70‡	2.20‡
Ethanol:Water (60)†	63.2 ± 2.1	119.8 ± 2.0	87.3 ± 1.9	32.5 ± 0.1	30.95‡	2.49‡
Ethylene glycol	80.1 ± 1.7	121.5 ± 2.0	95.4 ± 1.6	26.1 ± 0.4	47.76	16.06
Water	108.7 ± 2.3	134.5 ± 1.8	80.2 ± 1.5	54.3 ± 0.3	72.0	0.89

*Surface tension and viscosity collected from the literature at 25°C (*37*, *38*). †Percentage of ethanol in the mixture. ‡Surface tension and viscosity obtained from laboratory tests by our research group at 25°C.

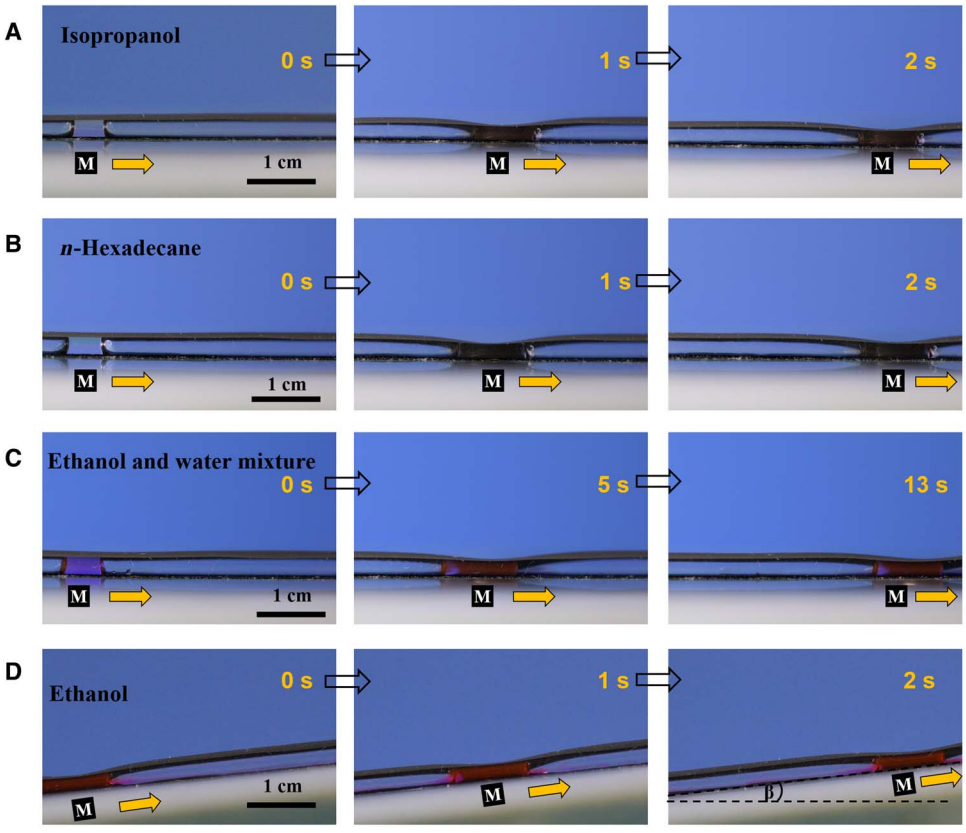

Fig. 3. Various magnetic-controlled liquid droplets in MTMAs. (**A** and **B**) Optical images showing magnetic-controlled motion of nonviscous liquids, including butyl alcohol, ethyl acetate, 1,2-dichloroethane, and *n*-hexadecane (movie S3). In all rows, the yellow arrows denote the magnet motion direction. (**C**) Optical images showing magnetic-controlled motion of a water and ethanol mixture. The mixture can be driven when the ethanol content is more than 60%, which corresponds to a CA of less than ~65° (movie S4). (**D**) Optical images showing magnetic-controlled motion of an ethanol droplet moving up an incline (movie S5).

be successfully manipulated. Table 1 lists the wetting behaviors on a PDMS film of a series of liquids with different surface tensions and viscosities. In our MTMAs, we investigated a wide range of partially wetting liquids, such as ethanol, ethyl acetate, hexadecane, isopropyl alcohol, and *n*-butyl alcohol (Fig. 3, A and B, and movie S3), and found that our MTMAs can successfully drive these liquids at different speeds. The specific details of magnetic-induced motion of water and ethanol mixture (ethanol, 80 volume %) are shown in Fig. 3C. It can be seen that the velocity of the droplet decreases with increasing water percentage (movie S4). This is to be expected, because larger amount of water makes the CAH increase (from 6.82 ± 0.4° to 17.3 ± 0.1°), reinforcing the pinning force. However, the droplet cannot be moved anymore when the water content is increased to 40%, corresponding to a CA of 63.2 ± 2.1°, which greatly broadens the range of the driven liquid (*36*). Droplet motion on a slope is more difficult than that on a horizontal surface because a large driving force is needed to overcome the resistance of the slope. As shown in Fig. 3D, our MTMAs can propel an ethanol droplet uphill on an incline with a speed of 1 cm s^{-1} (movie S5). Considering the effect of liquid swelling on devices, a stability test was carried out on the tensile performance of the MTMAs after every 100 uses in liquid transport. The fracture length and elastic modulus were found to be stable after ethanol droplet was transported 500 times (fig. S7, A and B). The swelling of PDMS by hexadecane was more serious than that by ethanol. However, in our MTMAs, the speed of the liquid transmission was much faster, allowing the hexadecane to be transported in a very short time. As shown in fig. S7 (C and D), after 300 cycles of liquid transport, the fracture length and elastic modulus began to decline. In addition, the movement of the liquid was synchronized with the switch in the magnet movement direction, and there was no hysteresis during a quick moving direction switch, whereas other methods based on external stimuli require a long period of time to change the liquid moving direction.

DISCUSSION

To better understand the droplet driving behavior, we next analyze the driving mechanism for liquid transport in the MTMAs. Figure 4 illustrates the liquid transport behavior in the MTMAs. A liquid drop in an MTMA with radius *r* forms menisci with angles θ_1 and θ_2 (Fig. 4A). Without the magnetic force, the two menisci are symmetric ($\theta_1 \approx \theta_2$), and the droplet is in a stationary state of mechanical equilibrium. When a magnetic force is applied, the soft tube will deform, causing a difference in the Laplace pressure ($\theta_R > \theta_A$), which will drive the droplet toward the narrower end (Fig. 4B). Figure 4C shows that the diameter of the tube at different positions declines with the increase of magnetic field (the closer the magnet, the greater the magnetic field), whereas the diameter of the tube at different positions without the magnetic field remains nearly constant. Therefore, the tube deforms to an asymmetric cone-like geometry, which generates an adjustable capillary force to propel the liquid in the direction of the

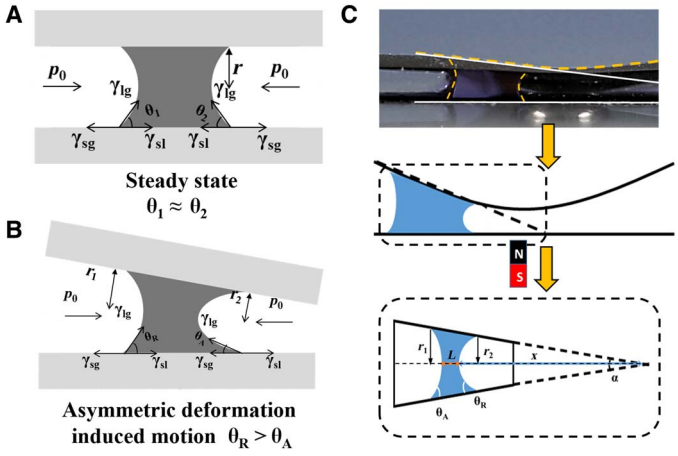

Fig. 4. Mechanism of the magnetic-controlled liquid transport behavior. Menisci formed by a liquid drop in an MTMA. (**A**) Steady state. (**B**) Conditions for droplet motion induced by the tube asymmetric deformation. (**C**) Snapshot of a droplet in its transport process and the correspondence between the true actuator and the simplified model.

magnet movement. The curvature variation of the menisci at each end of the liquid column and apex gives rise to a difference in the Laplace pressure (ΔP), which scales as (*22*, *23*)

$$\Delta P \approx (4\gamma\cos\theta)/\alpha x - (4\gamma\cos\theta)/\alpha(x+L) \approx (4\gamma L\cos\theta)/(ax\hat{}2) \quad (1)$$

where γ is the liquid surface tension, θ is the CA of the liquid, α is the apex angle, x is the distance of the precursor from the apex, and L is the length of the precursor. In our case, the distance between the liquid slug and the apex is much larger than the length of the liquid slug ($x \gg L$). Therefore, the capillary force (driving force, F_D) scales as (*22*, *23*)

$$F_D \approx \pi a\gamma L\cos\theta \quad (2)$$

This implies that the Laplace pressure on the precursor with a small curvature is always larger than that at the end of droplet with a large curvature; therefore, the resultant capillary force will drive the droplet to move toward the direction where the tube becomes narrower. If the magnet is fixed, the deformed section of tube is also fixed; the droplet will slowly move to find the mechanical equilibrium state again. Now, if we move the magnet to the right side (a very short distance), the deformed part of the tube will be relaxed as the imposed magnetic force becomes weaker. However, a new deformed section of tube forms, and the resultant capillary force pushes the droplet rightward. This indicates that if the magnet keeps moving, the droplet also moves following the magnet. One could imagine that there would be an upper velocity limit, above which the tube and droplet do not have enough time to deform, and the droplet will stop following the magnet.

The above discussion is valid for the case where the driving capillary force dominates. This is true for nonviscous and completely wetting liquids, as the resistant force there is negligible. As we all know, almost all liquids do not completely wet on a PDMS film. The liquid droplet motion is resisted by not only the viscous resistance (F_V) but also the adhesive force (F_A) arising from the CAH. The adhesive force is scaled as (*22*, *23*)

$$F_A \approx \gamma W\Delta\cos\theta \quad (3)$$

where W is the length of the advancing contact line, which is equal to πR, and R is the diameter of the MTMA. The term $\Delta\cos\theta = \cos\theta_R - \cos\theta_A$, where θ_R is the receding CA and θ_A is the advancing CA. The viscous resistance force is given by (*22*, *23*)

$$F_V \approx 8\pi\eta L\upsilon \quad (4)$$

where η is the coefficient of kinetic viscosity of the liquid and υ is the average speed of fluid motion.

Only when the capillary driving force is larger than the sum of the adhesive force and viscous resistance force can a partially wetting liquid be propelled. For nonviscous liquids, such as ethanol, isopropyl alcohol, ethyl acetate, and water, the CAH was previously regarded as a resistance force for liquid motion. In our case, the apex angle α of the MTMA is usually within the range of 0.07 to 0.17 according to the above calculation. We performed calculations for a series of low-viscosity liquids with various wettabilities (Table 1) and found that the threshold CA for droplet motion is approximately 63.2 ± 2.1°. The calculation results in table S2 agree well with the experimental results, which show that a less viscous liquid with a CA of less than ~65° in MTMAs can be propelled by magnetism (light blue area in Table 1). Our MTMAs greatly broaden the range of driven liquids without requiring further treatment of the surface to achieve complete wetting. It should also be pointed out that the actuation of a higher viscosity and more hydrophobic liquid with these MTMAs remains challenging (light yellow area in Table 1). Besides, due to the large driving force and instantaneous response of magnetism, our MTMAs can transport liquids at a relatively high speed. Based on the above discussion, an operating diagram is shown in fig. S8 for our result regarding the case of a 10-μl droplet. The diagram shows three distinct operating regions: steady droplet transport, magnet disengagement, and region in which the droplet cannot be driven.

In summary, we have developed a simple, effective, and low-cost strategy to fabricate asymmetric magnetic PDMS-based tubular microactuators. The MTMAs can successfully manipulate liquid motion with a magnet, generating an adjustable capillary force to propel a liquid toward the narrower end. Furthermore, the MTMAs do not require the addition of magnetic particles (content and properties); thus, MTMAs can better maintain the properties of transporting the droplets without contamination and can prevent the liquid from splitting from the magnetic particles or disengaging from the magnet. Moreover, lower-viscosity liquids with a CA of less than ~65° can be driven with controllable speed and direction, without further treatment of the MTMA inner wall to achieve complete wetting. The movement of the liquid droplet can be controlled up to a speed of 10 cm s^{-1}, which is, to our knowledge, a very high speed of liquid motion driven by a magnetic-induced capillary force in a closed tubular microactuator. We believe that the extended research related to tubular microactuators based on a magnetic force will shed new light on liquid manipulation, with a corresponding potential for wide applications.

MATERIALS AND METHODS

Preparation of the MTMAs

First, the Sylgard monomer PDMS 184 and the curing agent were mixed in a 1:10 ratio. This PDMS prepolymer was coated on the steel capillary with an outer diameter of 2 mm and kept in vertical direction at room temperature for 6 min, followed by thermal curing at 60°C for 20 min. Second, carbonyl iron powder (<10 μm) was added to the PDMS

prepolymer with vigorous stirring to form a mixture containing 70% iron powder. The compound was coated on clean glass slide using the tape-casting method, and the as-prepared film thickness was ~100 μm. Then, the previously obtained PDMS tube was carefully placed on the iron-doped PDMS prepolymer film, followed by secondary thermal curing at 80°C for 1 hour. Last, the whole tube was swelled in the hexane, the PDMS tube was quickly peeled off, and then the MTMAs were obtained.

Characterizations

All dynamic and static CAs were measured using the OCA 20 Contact Angle Measuring System (DataPhysics). A 2-μl liquid droplet was carefully deposited on the PDMS surfaces using a syringe. At least five different spots on the same sample surface were taken for CA measurements to receive a mean value. The viscosity properties of the mixed liquid were investigated using an Anton Paar model MCR-301 rheometer at 25°C. The surface tension properties of the mixed liquid were investigated using a high-sensitivity microelectromechanical balance system at 25°C.

SUPPLEMENTARY MATERIALS

Supplementary material for this article is available at http://advances.sciencemag.org/cgi/content/full/4/12/eaau8767/DC1

Fig. S1. The schematic procedure for preparing MTMA.
Fig. S2. The scanning electron microscopy images of obtained MTMAs.
Fig. S3. The plots of MTMA thicknesses.
Fig. S4. The scanning electron microscopy images of MTMA chosen in our experiment.
Fig. S5. The deformation of MTMAs with different diameters under magnetic field and the liquid droplet wetting property in MTMAs.
Fig. S6. Factors influencing the speed of droplet motion.
Fig. S7. Stability test of MTMAs after different numbers of liquid transport cycles.
Fig. S8. A phase diagram about the droplet motion.
Table S1. Comparison of various liquid driving systems.
Table S2. Calculation results for different forces on the probe liquids.
Movie S1. Driving liquid droplet in the MTMAs by asymmetric deformation.
Movie S2. Propelling different volume of liquid droplets by different velocities in MTMAs.
Movie S3. Various liquid droplets propelled by magnetic forces in MTMAs.
Movie S4. Magnetic-controlled water and ethanol mixture motion.
Movie S5. Magnetic-controlled droplet motion on an incline.

REFERENCES AND NOTES

1. E. K. Sackmann, A. L. Fulton, D. J. Beebe, The present and future role of microfluidics in biomedical research. *Nature* **507**, 181–189 (2014).
2. L. Ionov, N. Houbenov, A. Sidorenko, M. Stamm, S. Minko, Smart microfluidic channels. *Adv. Funct. Mater.* **16**, 1153–1160 (2006).
3. P. Liu, H. Zhang, W. He, H. Li, J. Jiang, M. Liu, H. Sun, M. He, J. Cui, L. Jiang, X. Yao, Development of "liquid-like" copolymer nanocoatings for reactive oil-repellent surface. *ACS Nano* **11**, 2248–2256 (2017).
4. K. AbuZineh, L. I. Joudeh, B. Al Alwan, S. M. Hamdan, J. S. Merzaban, S. Habuchi, Microfluidics-based super-resolution microscopy enables nanoscopic characterization of blood stem cell rolling. *Sci. Adv.* **4**, eaat5304 (2018).
5. D. Mark, S. Haeberle, G. Roth, F. Von Stetten, R. Zengerle, Microfluidic lab-on-a-chip platforms: Requirements, characteristics and applications, in *Microfluidics Based Microsystems. NATO Science for Peace and Security Series A: Chemistry and Biology* (Springer, 2010), pp. 305–376.
6. X. Hou, Y. S. Zhang, G. Trujillo-de Santiago, M. M. Alvarez, J. Ribas, S. J. Jonas, P. S. Weiss, A. M. Andrews, J. Aizenberg, A. Khademhosseini, Interplay between materials and microfluidics. *Nat. Rev. Mater.* **2**, 17016 (2017).
7. J. Charmet, P. Arosio, T. P. J. Knowles, Microfluidics for protein biophysics. *J. Mol. Biol.* **430**, 565–580 (2018).
8. M. Zarei, Advances in point-of-care technologies for molecular diagnostics. *Biosens. Bioelectron.* **98**, 494–506 (2017).
9. G. B. Celli, A. Abbaspourrad, Tailoring delivery system functionality using microfluidics. *Annu. Rev. Food Sci. Technol.* **9**, 481–501 (2018).
10. H. Li, P. Liu, G. Kaur, X. Yao, M. Yang, Transparent and gas-permeable liquid marbles for culturing and drug sensitivity test of tumor spheroids. *Adv. Healthc. Mater.* **6**, 1700185 (2017).
11. U. Lehmann, C. Vandevyver, V. K. Parashar, M. A. M. Gijs, Droplet-based DNA purification in a magnetic lab-on-a-chip. *Angew. Chem. Int. Ed. Engl.* **45**, 3062–3067 (2006).
12. F. Brochard, Motions of droplets on solid surfaces induced by chemical or thermal gradients. *Langmuir* **5**, 432–438 (1989).
13. D. Baigl, Photo-actuation of liquids for light-driven microfluidics: State of the art and perspectives. *Lab Chip* **12**, 3637–3653 (2012).
14. S.-K. Fan, P.-W. Huang, T.-T. Wang, Y.-H. Peng, Cross-scale electric manipulations of cells and droplets by frequency-modulated dielectrophoresis and electrowetting. *Lab Chip* **8**, 1325–1331 (2008).
15. Z. Long, A. M. Shetty, M. J. Solomon, R. G. Larson, Fundamentals of magnet-actuated droplet manipulation on an open hydrophobic surface. *Lab Chip* **9**, 1567–1575 (2009).
16. Y. Zhao, J. Fang, H. Wang, X. Wang, T. Lin, Magnetic liquid marbles: Manipulation of liquid droplets using highly hydrophobic Fe_3O_4 nanoparticles. *Adv. Mater.* **22**, 707–710 (2010).
17. Y. Zhang, N.-T. Nguyen, Magnetic digital microfluidics—A review. *Lab Chip* **17**, 994–1008 (2017).
18. J. Vialetto, M. Hayakawa, N. Kavokine, M. Takinoue, S. N. Varanakkottu, S. Rudiuk, M. Anyfantakis, M. Morel, D. Baigl, Magnetic actuation of drops and liquid marbles using a deformable paramagnetic liquid substrate. *Angew. Chem. Int. Ed. Engl.* **56**, 16565–16570 (2017).
19. J. V. I. Timonen, M. Latikka, L. Leibler, R. H. A. Ras, O. Ikkala, Switchable static and dynamic self-assembly of magnetic droplets on superhydrophobic surfaces. *Science* **341**, 253–257 (2013).
20. P. Wang, R. Bian, Q. Meng H. Liu, L. Jiang, Bioinspired dynamic wetting on multiple fibers. *Adv. Mater.* **29**, 1703042 (2017).
21. P. Renvoisé, J. W. M. Bush, M. Prakash, D. Quéré, Drop propulsion in tapered tubes. *Europhys. Lett.* **86**, 64003 (2009).
22. M. Prakash, D. Quéré, J. W. M. Bush, Surface tension transport of prey by feeding shorebirds: The capillary ratchet. *Science* **320**, 931–934 (2008).
23. J.-a. Lv, Y. Liu, J. Wei, E. Chen, L. Qin, Y. Yu, Photocontrol of fluid slugs in liquid crystal polymer microactuators. *Nature* **537**, 179–184 (2016).
24. J. M. Hill, An approximate load-deflection relation for a long half-cylindrical tube compressed between parallel plates. *Z. Angew. Math. Phys.* **28**, 169–175 (1977).
25. A. Van Hirtum, Deformation of a circular elastic tube between two parallel bars: Quasi-analytical geometrical ring models. *Math. Probl. Eng.* **2015**, 547492 (2015).
26. P.-G. de Gennes, F. B. Wyart, D. Quéré, *Capillarity and Wetting Phenomena* (Springer, 2004).
27. H. S. Khoo, F.-G. Tseng, Spontaneous high-speed transport of subnanoliter water droplet on gradient nanotextured surfaces. *Appl. Phys. Lett.* **95**, 063108 (2009).
28. M. Okochi, H. Tsuchiya, F. Kumazawa, M. Shikida, H. Honda, Droplet-based gene expression analysis using a device with magnetic force-based-droplet-handling system. *J. Biosci. Bioeng.* **109**, 193–197 (2010).
29. T. Wauer, H. Gerlach, S. Mantri, J. Hill, H. Bayley, K. T. Sapra, Construction and manipulation of functional three-dimensional droplet networks. *ACS Nano* **8**, 771–779 (2014).
30. Z. Cheng, L. Feng, L. Jiang, Tunable adhesive superhydrophobic surfaces for superparamagnetic microdroplets. *Adv. Funct. Mater.* **18**, 3219–3225 (2008).
31. K. Piroird, C. Clanet, D. Quéré, Detergency in a tube. *Soft Matter* **7**, 7498–7503 (2011).
32. T. Gu, C. Zheng, F. He, Y. Zhang, S. A. Khan, T. A. Hatton, Electrically controlled mass transport into microfluidic droplets from nanodroplet carriers with application in controlled nanoparticle flow synthesis. *Lab Chip* **18**, 1330–1340 (2018).
33. C. Dong, T. Chen, J. Gao, Y. Jia, P.-I. Mak, M.-I. Vai, R. P. Martins, On the droplet velocity and electrode lifetime of digital microfluidics: Voltage actuation techniques and comparison. *Microfluid. Nanofluid.* **18**, 673–683 (2015).
34. K. S. Seo, R. Wi, S. G. Im, D. H. Kim, A superhydrophobic magnetic elastomer actuator for droplet motion control. *Polym. Adv. Technol.* **24**, 1075–1080 (2013).
35. J. Jeon, J.-B. Lee, S. K. Chung, D. Y. Kim, On-demand magnetic manipulation of liquid metal in microfluidic channels for electrical switching applications. *Lab Chip* **17**, 128–133 (2017).
36. M. Liu, S. Wang, L. Jiang, Nature-inspired superwettability systems. *Nat. Rev. Mater.* **2**, 17036 (2017).
37. C. L. Yaws, *Chemical Properties Handbook* (McGraw-Hill Co., 1999).
38. I. M. Smallwood, *Handbook of Organic Solvent Properties* (Arnold, 1996).

Acknowledgments

Funding: This research was supported by the National Research Fund for Fundamental Key Projects (2017YFA0204504), National Natural Science Funds for Distinguished Young Scholar (No. 21725401), National Key R&D Program of China (No. 2017YFA0207800), and the National Natural Science Foundation (21722309 and 21671194). **Author contributions:** Y.T. and L.J. conceived and supervised the project. W.L., G.H., and M.L. designed the experiments and

contributed equally to this work. W.L. and Q.R. performed some of the experiments. W.L. wrote the manuscript. Y.X., M.L., L.J., and Y.T. participated in the discussion. W.L., M.L., and Y.T. revised the manuscript. All authors discussed the results and commented on the manuscript. **Competing interests:** The authors declare that they have no competing interests. **Data and materials availability:** All data needed to evaluate the conclusions in the paper are present in the paper and/or the Supplementary Materials. Additional data related to this paper may be requested from the authors.

Submitted 23 July 2018
Accepted 19 November 2018
Published 21 December 2018
10.1126/sciadv.aau8767

Citation: W. Lei, G. Hou, M. Liu, Q. Rong, Y. Xu, Y. Tian, L. Jiang, High-speed transport of liquid droplets in magnetic tubular microactuators. *Sci. Adv.* **4**, eaau8767 (2018).

Science Advances

High-speed transport of liquid droplets in magnetic tubular microactuators

Wenwei Lei, Guanglei Hou, Mingjie Liu, Qinfeng Rong, Yichao Xu, Ye Tian and Lei Jiang

Sci Adv **4** (12), eaau8767.
DOI: 10.1126/sciadv.aau8767